Molecular Crystals and Liquid Crystals

ISSN: 1542-1406 (Print) 1563-5287 (Online) Journal homepage: http://www.tandfonline.com/loi/gmcl20

Accurate Modelling of Liquid Crystal-Based Microwave Devices

F. A. Fernández, L. Seddon, R. James, S. E. Day, S. Bulja, P. Deo & D. Mirshekar-Syahkal

To cite this article: F. A. Fernández, L. Seddon, R. James, S. E. Day, S. Bulja, P. Deo & D. Mirshekar-Syahkal (2015) Accurate Modelling of Liquid Crystal-Based Microwave Devices, Molecular Crystals and Liquid Crystals, 619:1, 19-27, DOI: 10.1080/15421406.2015.1087271

To link to this article: http://dx.doi.org/10.1080/15421406.2015.1087271

Published online: 23 Oct 2015.

Mol. Cryst. and Liq. Cryst., Vol. 619: pp. 19–27, 2015

ISSN: 1542-1406 print/1563-5287 online
DOI: 10.1080/15421406.2015.1087271

Accurate Modelling of Liquid Crystal-Based Microwave Devices

F. A. FERNÁNDEZ,[1,*] L. SEDDON,[1] R. JAMES,[1] S. E. DAY,[1] S. BULJA,[2] P. DEO,[2] AND D. MIRSHEKAR-SYAHKAL[2]

[1]University College London, London, UK
[2]University of Essex, Colchester, UK

Liquid crystal substrates have been shown to provide the means to develop low-cost, reconfigurable, adaptive and tuneable microwave devices for mobile and wireless communication systems. In order to take maximum advantage of the possibilities that these materials offer and to design LC-based devices appropriately, techniques for the characterisation of the liquid crystal dielectric properties are needed. Similarly, appropriate modelling methods are required to simulate accurately the switching behaviour of the liquid crystal and the characteristics of the wave propagation through the devices, taking full consideration of the point-by-point variation of the material tensor permittivity.

Keywords Liquid crystals; microwave devices; tuneable microwave devices; reconfigurable microwave devices

Introduction

Recent mobile and wireless communication systems as well as modern radars require reconfigurable filters, tuneable and adaptive antennas, adaptive couplers, electronically controlled delay-lines, etc., in order to be flexible and operational under different communication standards and environmental conditions. Also, for security reasons, lightweight field radios and radar systems are required to reconfigure and operate over different frequency bands in a short time span. Research has shown that liquid crystals (LCs) are particularly attractive for these applications. As in the optical range, liquid crystals offer the possibility of large permittivity changes, controlled by low, externally applied voltages, so their incorporation as substrates in microwave devices provides a low-cost solution to the problem of achieving tuneable, adaptive or reconfigurable systems. Some of the LC-based devices reported in the literature are tunable microstrip patch antennas, variable phase shifters, reflect arrays, beam steering antennas, filters and tunable resonators and filters [1–11]. These devices use nematic liquid crystals which are relatively cheap, respond to low voltages, and are highly linear under large RF fields [12]. They offer various advantages over piezoelectrics and ferroelectrics [13, 14] in many RF applications in spite of their slower response time.

*Address correspondence to F. A. Fernández, University College London, London, UK. E-mail: a.fernandez@ucl.ac.uk

Color versions of one or more of the figures in the article can be found online at www.tandfonline.com/gmcl.

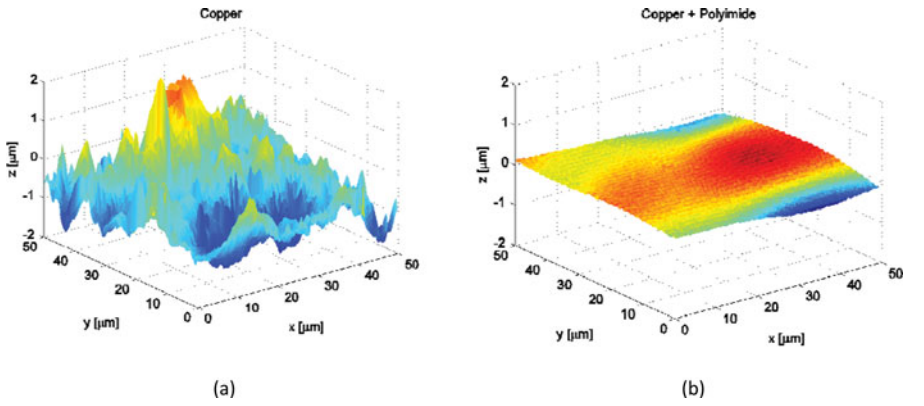

Figure 1. Atomic Force Microscopy images of (a) untreated and (b) planarised Rogers TMM3 microwave substrate.

To take full advantage of these possibilities and design devices effectively, it is necessary to explore the opportunities offered by liquid crystals thoroughly, with a full characterisation of the materials at the frequencies involved. It is also important to develop accurate modelling techniques that can predict the behaviour of LC materials in complex device configurations and can take into account the full anisotropy and non-uniformity of its permittivity distribution in the modelling of the RF operation of the device. The LC properties can be controlled by changing the components in the mixtures, but in order to formulate the mixtures properly the properties must be measured over the relevant frequency ranges.

We have developed techniques that combine LC modelling, electromagnetic modelling and experimental measurements for the wide-band characterisation of LC materials at microwave frequencies and for the analysis and design of complex LC-based, reconfigurable and tuneable microwave devices.

These methods have been used to design and analyse microwave filters, resonators and phase shifters for phased antenna arrays and can be equally well applied in other frequency ranges including terahertz and optics.

Device Fabrication Issues

The design and fabrication of LC devices at microwave frequencies present some different challenges to those encountered in optical devices. Common microwave substrate materials for planar devices have high surface roughness and hence they need to be especially treated and planarized in order to provide an effective anchoring and alignment surface for the LC. Fig. 1 shows atomic force microscopy (AFM) images of Rogers TMM3 microwave substrate untreated and planarised using a thick layer (about 3 μm) of polyimide. Fig. 1(a) shows the untreated substrate with surface roughness of 2 μm. Fig. 1(b) shows the roughness reduced to less than 0.2 μm after being coated with a thick layer of polyimide. Effective anchoring can now be provided by rubbing [15]. However, to take maximum advantage of the liquid crystal anisotropy in designing complex devices, other anchoring methods, like photo-alignment, can be more appropriate [16]. For example, if the device consists of curved lines as in a meander line phase shifter or in a ring resonator, it would be advantageous that

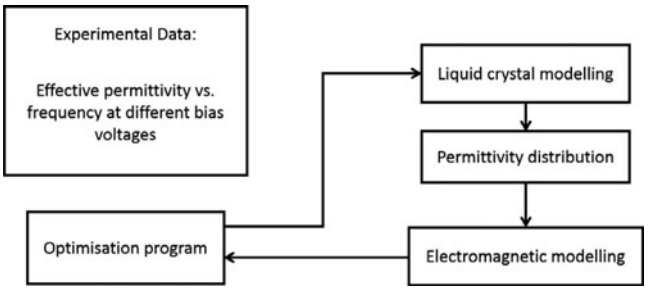

Figure 2. Schematic procedure for the broadband characterisation of liquid crystal materials.

the liquid crystal alignment follows the bends of the line so the liquid crystal switching would provide maximum anisotropy throughout the length.

The thickness of the conducting lines (electrodes) is another issue that can cause problems with the liquid crystal anchoring and alignment. For example, in the common microwave substrate series Rogers TMM3, the copper layer is around 17 μm thick and after etching, the sides of the lines are of higher roughness than the top surface of the copper layer. Although a thick layer of polyimide cannot make these sides planar, it provides sufficient smoothness to avoid alignment problems.

Other issues that arise in the design of LC-based microwave devices are related to the thickness of the liquid crystal layer. In order to achieve the desirable characteristic impedance for the lines, and depending of the frequency of operation, the thickness of the liquid crystal layer often needs to be of around 100 μm or more, which for common liquid crystal devices is very large. This could cause some problems for the liquid crystal alignment and will make the device slow to switch. This is not an issue for many tuneable or reconfigurable devices where response times of around tens or hundreds of milliseconds are acceptable, but this technology is inappropriate for fast modulators or other devices that require rapid response times.

Broadband Characterization Method

Conventional methods used in optics for the characterisation of liquid crystals are not practical due to the much larger cell thickness required in the microwave bands and hence complex experimental equipment and specialised devices have been used [1, 17]. Methods based on resonant structures have been used for the characterisation of LC materials at single frequencies [18–21]. A method for the broadband characterisation of LC materials was presented and used in [22–24]. The method is based on an optimisation approach using experimental results for the effective permittivity of a planar transmission line section, combined with liquid crystal and electromagnetic modelling. Schematically, the procedure is represented in Fig. 2.

Using a simple device consisting of a section of a stripline and two matching feed sections, and measuring it with a vector network analyser, the effective permittivity of the microstrip section can be extracted over a frequency range for a set of different voltage levels corresponding to different degree of switching of the liquid crystal substrate. An optimisation procedure is then set up for the parallel and perpendicular permittivities of the liquid crystal that use liquid crystal modelling to find the director distribution and hence, the tensor permittivity distribution over the device cross-section. This is then used by an

electromagnetic modal analysis program that finds the corresponding values of the effective permittivity which are compared with the experimental results at two voltage values. Using data obtained at more voltage values, additional parameters of interest of the liquid crystal can be found, for example the elastic constants [23]. Similarly, if experimental data for the effective loss tangent is used, the parallel and perpendicular loss tangent of the liquid crystal can be found [23, 24].

Since defects in the liquid crystal ordering are not important in such large structures, unless they cause large-scale alignment problems, the liquid crystal modelling used in these calculations is based on the Ossen-Frank formulation, that is, the liquid crystal orientation is found by minimising the energy functional:

$$\mathcal{F} = \int_{\Omega} \{f_D - f_E\} \quad d\Omega + \int_{\Gamma} \{f_S\} \quad d\Gamma \tag{1}$$

where

$$f_D = \frac{1}{2}K_{11}(\nabla \cdot \hat{n})^2 + \frac{1}{2}K_{22}(\hat{n} \cdot \nabla \times \hat{n} + q_0)^2 + \frac{1}{2}K_{33}(\hat{n} \times \nabla \times \hat{n} + q_0)^2 \tag{2}$$

$$f_E = \frac{1}{2}\varepsilon_0(\vec{E} \cdot \bar{\bar{\varepsilon}}_r \cdot \vec{E}) \tag{3}$$

are the elastic distortion and electric energies respectively and f_S is the surface anchoring energy [25]. The electric field is found by the minimisation of the electric functional:

$$F_E = \int_{\Omega} \{f_E\} d\Omega \tag{4}$$

and the solution is obtained using the finite elements method.

The electromagnetic modelling of the waveguide modes used to find the effective permittivity is based on the variational form:

$$J(\vec{E}) = \frac{1}{2}\int_{\Omega} \left\{ \frac{1}{\mu_r}(\nabla \times \vec{E}) \cdot (\nabla \times \vec{E})^* - k_0^2 \vec{E} \cdot \bar{\bar{\varepsilon}}_r \cdot \vec{E} \right\} d\Omega \tag{5}$$

Using $\vec{E}(x, y, z) = \vec{E}(x, y)e^{-jkz}$, the variational form (5) becomes:

$$\begin{aligned} J(\vec{E}) = \frac{1}{2}\int_{\Omega} \Bigg\{ & \frac{1}{\mu_r}(\nabla_t \times \vec{E}_t) \cdot (\nabla_t \times \vec{E}_t)^* - k_0^2 \vec{E}_t \cdot \bar{\bar{\varepsilon}}_r \cdot \vec{E}_t \\ & + \frac{1}{\mu_r}(\nabla_t E_z + jk_z \vec{E}_t) \cdot (\nabla_t E_z + jk_z \vec{E}_t)^* \Bigg\} d\Omega \end{aligned} \tag{6}$$

which results in a quadratic eigenvalue equation for the propagation constant k_z.

For the most general case of LC orientations, giving a full permittivity tensor, the resultant eigenvalue problem can be linearized in the form:

$$\begin{pmatrix} 0 & I & 0 \\ A_{tt} & 0 & -jC_{tz} \\ 0 & jC_{tz} & 0 \end{pmatrix} \begin{pmatrix} e_t \\ k_z e_t \\ k_z e_z \end{pmatrix} = k_z \begin{pmatrix} I & 0 & 0 \\ 0 & B_{tt} & B_{tz} \\ 0 & B_{tz}^T & B_{zz} \end{pmatrix} \begin{pmatrix} e_t \\ k_z e_t \\ k_z e_z \end{pmatrix} \tag{7}$$

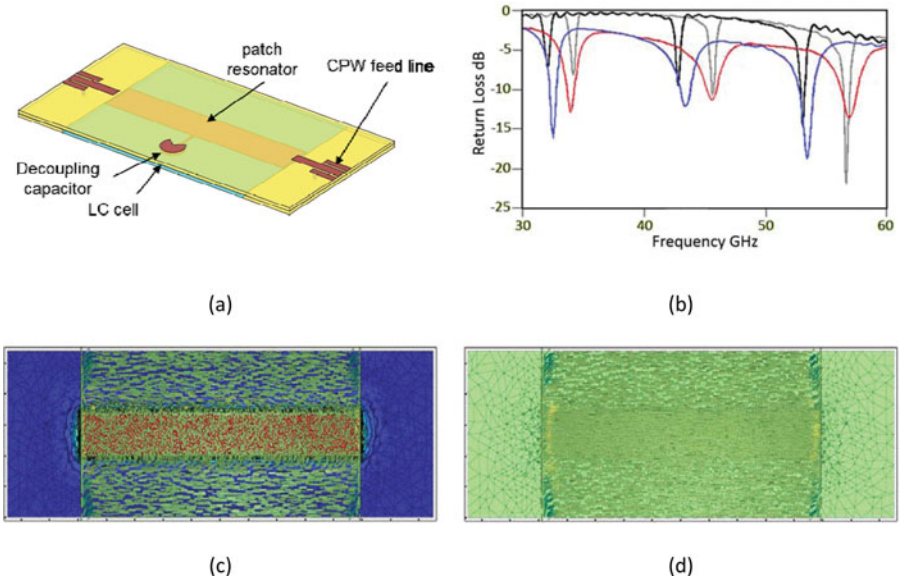

Figure 3. (a) A simple long patch resonator with liquid crystal substrate, (b) modelled (black and grey) and measured return losses (blue and red) for the switched (black and blue) and unswitched (grey and red) cases. Liquid crystal director distributions in (c) switched and (d) unswitched states.

where $\vec{e}_t = k_z \vec{E}_t$ and $e_z = -jE_z$. The solution is implemented using finite elements, with a combination of edge elements for $\vec{e}_t$ and nodal elements for e_z.

Propagation Analysis

An accurate modelling of the electromagnetic propagation through a device containing liquid crystal substrates is necessary to study the effects of the switching behaviour of the liquid crystal on the different field components and optimise the device design. The method developed here is a scattering approach that is based on a variational form of the Helmholtz equation and can find the full electromagnetic field in a device, or in specified ports, when an excitation field is applied.

The device is assumed to be contained in a region which is bounded by either metal walls or absorbing boundary conditions. Additionally, radiation can also be allowed by treating the exterior region as boundary elements (Green's functions), at the expense of a much greater computing time.

The variational expression used for the case of only two ports is [26]:

$$\begin{aligned} K(\vec{E}) = \frac{1}{2}\int_{\Omega}\left\{\frac{1}{\mu_r}(\nabla\times\vec{E})\cdot(\nabla\times\vec{E})^* - k_0^2\vec{E}\cdot\bar{\bar{\varepsilon}}_r\cdot\vec{E}\right\}d\Omega \\ + \sum_{k=1}^{2}\int_{S_k}\left\{\frac{jk_0}{2}(\hat{n}\times\vec{E})\cdot(\hat{n}\times\vec{E})^* + \vec{E}_t\cdot U_k^{inc}\right\}dS \\ + \int_{\Gamma\setminus\cup S_k}\left\{\frac{jk_0}{2}(\hat{n}\times\vec{E})\cdot(\hat{n}\times\vec{E})^*\right\}dS \end{aligned} \tag{8}$$

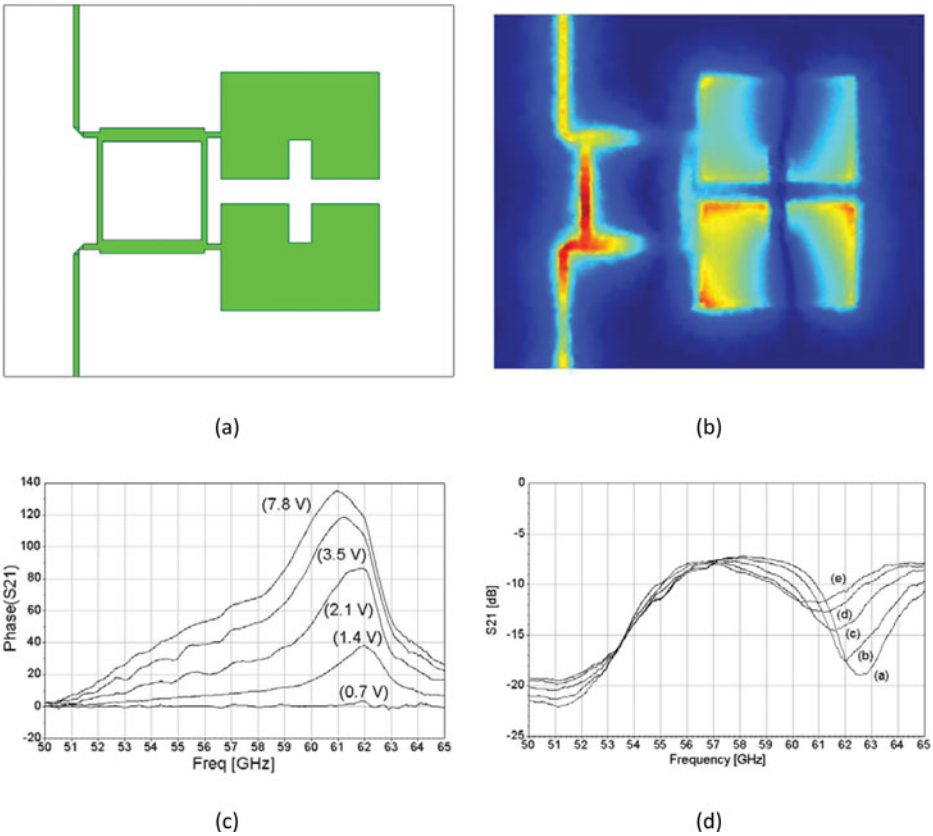

Figure 4. Results for a reflection-type phase shifter. (a) Schematic outline of the top layer, (b) electric field distribution, (c) differential phase shift for different applied voltages, and (d) insertion losses for different applied voltages.

The excitation vectors U_k^{inc} are determined from the modal fields at the ports. Again, a combination of liquid crystal and electromagnetic modelling, implemented with finite elements is used to find the full electromagnetic fields in the structure. The permittivity distribution over the liquid crystal layer is found first using a 3D version of (1)–(4) and these are then mapped over the tetrahedral mesh for the complete structure. The modal analysis described in (5)–(7) is used to find the modal fields at the ports and to determine the corresponding scattering parameters.

Results

The methods described above have been used to study a number of devices. Figure 3(a) shows a simple long patch resonator 7.84 mm long over a solid aluminium ground plane. The space between the top layer (superstrate) and the ground plane, 101 μm thick is filled with liquid crystal, which is switched by means of a low frequency voltage applied between the ground plane and the patch resonator. The modelled and measured return losses for the switched and unswitched states of the liquid crystal are shown in Fig. 3(b). Dielectric losses were not considered in the modelled results and that causes the magnitude (vertical) shift

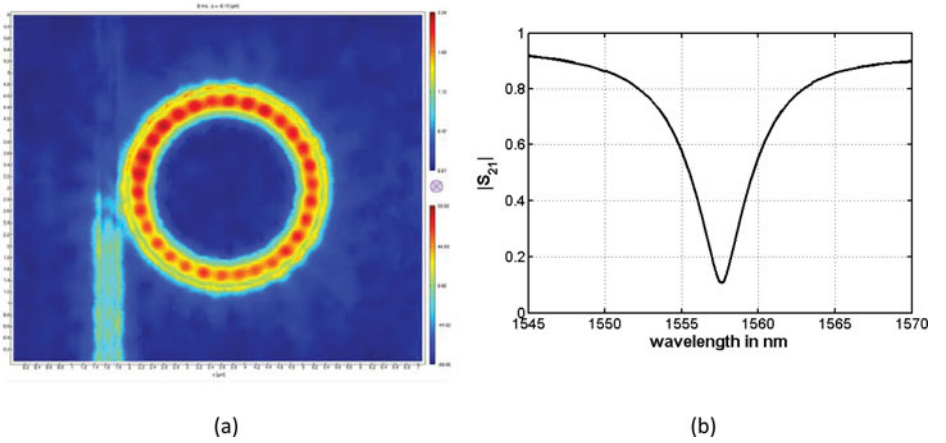

Figure 5. An optical ring resonator. (a) Field distribution at resonance, and (b) transmittance versus wavelength in the unswitched state.

observed in the frequency response. There is good agreement in the resonant frequencies between the experimental results and the modelling.

Figure 4 shows results for a reflection-type phase shifter [27]. The outline of the top layer including the input and output lines and the resonators is shown in (a). This metal layer also acts as the top electrode to apply the switching voltage across the liquid crystal layer. The electric field distribution at 65 GHz on a plane inside the liquid crystal layer is shown in Fig. 4(b). The differential phase shift with respect to the unswitched state (0 V) and the insertion losses are shown in Fig. 4(c) and 4(d) respectively, for a range of different states of switching of the liquid crystal substrate, corresponding to different voltages applied between the top and ground electrodes.

The modelling techniques developed here not only are applicable to the microwave range of frequencies but can also be used in the terahertz region and in optics. As an example, Fig. 5 shows modelling results for an optical ring resonator. The guide and the ring are segments of a rib waveguide of 290 nm by 250 nm and refractive index 11.7, over a substrate of refractive index 3.9 with the liquid crystal as a cladding. The field distribution on a plane within the liquid crystal cladding is shown in Fig. 5(a) at resonance, which occurs at a wavelength of 1557.6 nm. Fig. 5(b) shows the transmittance versus wavelength for the unswitched state.

Conclusions

We have presented accurate modelling techniques for the characterisation of liquid crystal materials in the microwaves range and to study electromagnetic wave propagation through devices containing liquid crystal substrates. This allows the efficient design of LC-based microwave devices tacking full advantage of the liquid crystal externally controlled anisotropy. The permittivity data for the electromagnetic solvers is calculated by an accurate liquid crystal modelling method based on the minimization of the free energy. For the characterisation, the test device is based on a uniform stripline and a 2D modal analysis is used to determine the effective permittivity (or propagation constant) from which the relevant parameters of the liquid crystal material can be found. For the modelling of devices, a 3D

scattering software has been implemented, that use the 3D (tensor) permittivity distribution over the liquid crystal layer found by LC modelling, to calculate EM fields over the whole structure and scattering parameters at defined ports. Results of the applications of the modelling techniques for different examples were presented and verified by measurements. The extension of the modelling to THz and optical devices containing liquid crystal as substrate is straightforward and this is demonstrated by an example.

Funding

This work has been funded by the UK Engineering and Physical Sciences Research Council, EPSRC.

References

[1] Kuki, T., Fujikake, H. & Nomoto, T. (2002). *IEEE Trans. Microw. Theory Tech.*, *50*(11), 2604–2609.
[2] Fritzsch, C., Giacomozzi, F., Karabey, O.H., Bildik, S., Colpo, S. & Jakoby, R. (2012). *Int. J. Microwave Wireless Tech.*, *4*, 379–386.
[3] Martin, N., Laurent, P., Person, C., Gelin, P. & Huret, F. (2003). *Proceedings European Microwave Conference (EUMC), Munich, Germany*, 699–702.
[4] Hu, W., Cahill, R., Encinar, J.A., Dickie, R., Gamble, H., Fascco, V. & Grant, N. (2008). *IEEE Trans. Antennas Propagat.*, *56*, 3112–3117.
[5] Doumaines, E. *et al.* (2013). *Proceedings European Conference on Antennas and Propagation. (EUCAP), Gothenburg, Sweden*, 1791–1792.
[6] Gaebler, A. *et al.* (2009). *Int. J. Antennas Propag.*, *2009*, Article ID 876989.
[7] Fusco, V.F., Cahill, R., Hu, W. & Simms, S. (2008). *Electron. Lett.*, *44*(1), 37–38.
[8] Yaghmaee, P. *et al.* (2012). *Electron. Lett.*, *48*(13), 798–800.
[9] Yazdanpanahi, M. & Mirshekar-Syahkal, D. (2012). *Proceedings IEEE Radio Wireless Symp. (RWS), Santa Clara, California, USA*, 139–142.
[10] Perez-Palomino, G. *et al.* (2014). *IEEE Trans. Anntenas Propagat.*, *62*(5), 2659–2668.
[11] Torrecilla, J. *et al.* (2013). *Microwave Opt Technol Lett*, *55*(10), 2420–2423.
[12] Goelden, F. *et al.* (2006). *Proceedings European Microwave Conference (EUMC), Manchester, UK*, 971–974.
[13] Giere, A., Scheele, P., Zheng, Y. & Jakoby, R. (2007). *IEEE Microw. Wireless. Compon. Lett.*, *17*(6), 442–444.
[14] Poplavko, *et al.* (2006). *Proceedings European Microwave Conference (EUMC), Manchester, UK*, 657–660.
[15] Ishihara, S. (2005). *IEEE/OSA J. Display Technol.*, *1*(1), 30–40.
[16] Chigrinov, V.G. *et al.* (2008). *Photoalignment of Liquid Crystalline Materials: Physics and Applications*, John Wiley & Sons, Ltd.
[17] Yang, F. & Sambles, J.R. (2002). *Appl. Phys. Lett.*, *81*(11), 2047–2049.
[18] Yazdanpanahi, M. (2012). *Liquid Crystal Measurements and Devices at Milimetre-wave Frequencies*, University of Essex, UK.
[19] Yazdanpanahi, Bulja, M.S., Mirshekar-Syahkal, D., James, R., Day, S.E. & Fernández, F.A. (2010). *IEEE Trans. Instrumentation and Measurements*, *59*(12), 3079–3085.
[20] Utsumi, Y. *et al.* (2004). *Mol. Cryst. Liq. Cryst.*, *409*, 355–370.
[21] Das, N.K. *et al.* (1987). *IEEE Trans. Microw. Theory Tech.*, *35*(7), 636–641.
[22] James, R., Fernández, F.A., Day, S.E., Bulja, S., Yazdanpanahi, M. & Mirshekar-Syahkal, D. (2009). *IEEE Trans. Microw. Theory Tech.*, *57*(12), 3393–3397.
[23] James, R., Fernández, F.A., Day, S.E., Bulja, S. & Mirshekar-Syahkal, D. (2011). *Mol. Cryst. Liq. Cryst.*, *542*(1), 196[718]-203[725].

[24] Bulja, S., Yazdanpanahi, M., Mirshekar-Syahkal, D., James, R., Day, S.E. & Fernández, F.A. (2010). *IEEE Trans. Microw. Theory Tech.*, *58*(12), 3493–3501.
[25] Zhao, W., Wu, C.-X. & Iwamoto, M. (2000). *Phys. Rev. E*, *62*(2), 1481–1484.
[26] Jin, J. (1993). *The Finite Element Method in Electromagnetics*, J. Wiley, N.Y.
[27] Kim, D., *et al.* (2002). *IEEE Trans. Microw. Theory Tech.*, *50*(12), 2903–2909.